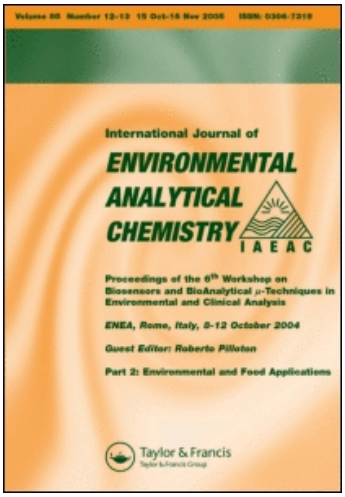

International Journal of Environmental Analytical Chemistry
Publication details, including instructions for authors and subscription information:
http://www.informaworld.com/smpp/title~content=t713640455

Application of response surface methodology for modelling the enzymatic assay of hydrogen peroxide by Emerson-Trinder reaction using 4-iodophenol

Farzad Deyhimi[a]; Rahman Salamat-Ahangari[a]; Massood Arabieh[a]; Lida Parvin[a]
[a] Department of Chemistry, Shahid Beheshti University, Evin-Tehran 19839, Iran

To cite this Article Deyhimi, Farzad , Salamat-Ahangari, Rahman , Arabieh, Massood and Parvin, Lida(2006) 'Application of response surface methodology for modelling the enzymatic assay of hydrogen peroxide by Emerson-Trinder reaction using 4-iodophenol', International Journal of Environmental Analytical Chemistry, 86: 15, 1151 — 1163
To link to this Article: DOI: 10.1080/03067310600739673
URL: http://dx.doi.org/10.1080/03067310600739673

Intern. J. Environ. Anal. Chem.
Vol. 86, No. 15, 20 December 2006, 1151–1163

Taylor & Francis
Taylor & Francis Group

Application of response surface methodology for modelling the enzymatic assay of hydrogen peroxide by Emerson–Trinder reaction using 4-iodophenol

FARZAD DEYHIMI*, RAHMAN SALAMAT-AHANGARI, MASSOOD ARABIEH and LIDA PARVIN

Department of Chemistry, Shahid Beheshti University, Evin-Tehran 19839, Iran

(*Received 9 January 2006; in final form 24 March 2006*)

In this work, an initial-rate spectrophotometric method and response surface methodology (RSM) were combined for modelling and optimizing the experimental parameters of the enzymatic Emerson–Trinder reaction, for the determination of hydrogen peroxide. This spectrophotometric indicator reaction is currently used in biotechnology for the determination of phenolic compounds (e.g. in industrial samples) and also for determination of various substrates (e.g. in clinical chemistry). Using 4-iodophenol as a hydrogen donor in this reaction, the quality of the generated second-order polynomial response model equation was checked by the kinetic assay of H_2O_2 in real samples (e.g. cosmetic and human pooled serum samples), where their resulting satisfactory analytical characteristics were reported.

Keywords: Horseradish peroxidase; Response surface methodology; Hydrogen peroxide; 4-Iodophenol; Emerson–Trinder reaction; Initial rate

1. Introduction

In 1969, Trinder [1, 2] modified the colour test reaction, previously reported by Emerson [3], by using horseradish peroxidase (HRP) enzyme for the determination of blood glucose. Initially, the Emerson non-enzymatic reaction [3] was designed as a new colour test reaction for the determination of phenolic compounds [4]. Effectively, Trinder coupled the oxidizing hydrogen peroxide, produced in the glucose/glucose oxidase reaction, to the indicator Emerson reaction. That is why this reaction, also known as the Trinder reaction, is nowadays still in common use in many field of biotechnology for the determination of phenolic compounds [4–6] and is also routinely used as a spectrophotometric indicator reaction in clinical chemistry. Moreover, this indicator reaction was also exploited for the spectrophotometric assay of a large number of substrates or enzymes [7] such as uric acid [8], cholesterol [9], free haemoglobin [10], or triglycerides [11], and also by using different organic hydrogen-donor compounds such as different substituted (*ortho*, *meta* and *para*) chloro

*Corresponding author. Fax: +98-21-22403041. Email: f-deyhimi@cc.sbu.ac.ir

International Journal of Environmental and Analytical Chemistry
ISSN 0306-7319 print/ISSN 1029-0397 online © 2006 Taylor & Francis
DOI: 10.1080/03067310600739673

or bromophenols, 4-hydroxybenzene-sulphonic acid [12], 2,4-dichlorophenol [13], 3,5-dichloro-2-hydroxybenzensulphonic acid [11, 14] or different aniline derivatives [15]. Recently, the ability of this reaction was also exploited as a 'potentiometric' indicator reaction for the assay of hydrogen-peroxide-generating systems, by using a fluoride ion-selective electrode to monitor the rate of fluoride ion produced in the HRP-catalysed oxidative condensation of 4-fluorophenol with 4-aminoantipyrine (4-AAP) by hydrogen peroxide. As a result, the corresponding potentiometric method and its analytical capability for the assay of uric acid, in aqueous and serum samples, have been reported [16].

Using 4-iodophenol as H donor, it seemed useful to optimize the experimental parameters involved in this reaction by a powerful chemometric method such as Response Surface Methodology (RSM), in view of the significant versatility of this indicator reaction.

2. Experimental

2.1 *Chemicals*

All experiments were performed using solutions prepared from analytical-grade chemicals and doubly distilled water. The enzyme horseradish peroxidase (HRP, hydrogen peroxide oxidoreductase; EC 1.11.1.7) was purchased from Boehringer-Manheim (Germany), and all other compounds were obtained from Merck (Germany). Different tris(hydroxymethyl-aminomethane) solutions (tris-buffer) were prepared with the following concentrations: 50, 100, 150, 200, and 250 mM, and their pHs were adjusted before use according to the values indicated in the experimental design table. Initial fresh solution of 4-iodophenol (4-IP) 2.50 mM was prepared each time by dissolving in acetone. Stock solutions of 200 mM 4-aminoantipyrine (4-AAP) were prepared in the appropriate tris-buffer solutions. The initial solution of HRP enzyme ($5.902\,\mathrm{kU\,L^{-1}}$) was also freshly prepared before each series of measurements. The activity of HRP enzyme stock solution was determined according to a standard procedure [17]. The appropriate volume of 4-APP was added each time to achieve the final concentration indicated in the experimental design table. The stock and calibration solutions of H_2O_2 were also prepared directly by dilution of the original reagent grade Merck solution, and its concentration was determined by a spectrophotometric method (at $\lambda = 230\,\mathrm{nm}$, $\varepsilon_{230\,\mathrm{nm}} = 72.7\,\mathrm{M\,cm^{-1}}$) [18].

2.2 *Real samples*

Both human pooled serum and cosmetic samples were used to check the quality of the improvement of the enzymatic indicator reaction by the assay of H_2O_2. The ordinary cosmetic samples used for validation of the optimized reaction (scheme 1) performances consisted of three different peroxide oxidant hair-bleaching creams and lotion with the following declared qualitative compositions:

- Sample 1 (S1): stearyl alcohol, H_2O_2 (9% w/w), herbal essences, additives (Welloxon oxidant cream produced under the license by Wella AG, Darmstadt, Germany);

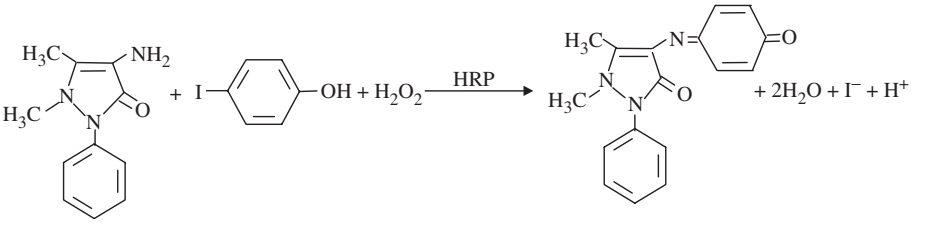

Scheme 1. Emerson–Trinder reaction using 4IP.

- Sample 2 (S2): H_2O_2 (9%), cetyl alcohol, GMS (glyceryl monostearate) emulsifying compounds, colourant, and additives (Atousa oxidant cream produced by Sabz-Golsar Co., Iran);
- Sample 3 (S3): H_2O, H_2O_2 (6%), stearyl alcohol, sodium stearyl sulphate, PEG-40 Castor oil, disodiumpyrophosphate, disodium EDTA, sodium benzoate, phosphoric acid, perfume (Igora Oxygenta lotion produced under license by Hans Schwarzkopf GmbH & Co., KG, Hamburg, Germany).

2.3 *Instrumentation*

The experimental absorption data were obtained using quartz cells ($l = 1$ cm) and a Shimadzu UV-Vis spectrophotometer (model 2100, Japan) equipped with a thermostat and interfaced with a personal computer for data acquisition and processing. The pH of the solutions was adjusted using a combined pH electrode and pH meter (model 691), both from Metrohm (Switzerland).

3. Principle of the method

3.1 *Indicator reaction*

The principle of the three substrates enzymatic Emerson–Trinder reaction, presented below (see scheme 1), is based on the formation of a red-purple-coloured quinoneimine dye, produced by oxidative condensation of a phenolic compound with 4-AAP by hydrogen peroxide, and catalysed by HRP enzyme.

The collection of the experimental absorption data was performed at the maximum of the absorption band of the produced quinoneimine complex ($\lambda_{max} = 505$ nm). The calculation was based on the initial rate method (e.g. variation of absorbance at λ_{max} *vs.* time).

Although the spectrophotometric assay of H_2O_2 can simply be determined at the end of reaction by the resulting increase in absorption (end-point measurement) due to the production of the coloured complex, the following more rapid and efficient initial-rate method could also be used according to the following first-order rate equation:

$$r = \left(\frac{\mathrm{d[Abs]}}{\mathrm{d}t}\right)_{\mathrm{init}} = k_{\mathrm{exp}}[H_2O_2]. \quad (1)$$

In the above relation, the initial rate is directly proportional to the slope of the progress curve at the beginning of the reaction, which can be started by the addition of HRP enzyme into the reagent mixture.

3.2 *Chemometric procedure*

Using the initial-rate method for the determination of hydrogen peroxide, the corresponding critical variables and their ranges were first determined based on a preliminary 'one variable at a time' (OVAT) approach. Further optimization was then carried out using response surface methodology (RSM). In fact, RSM is a collection of mathematical and statistical techniques that are useful for the modelling and analysis of processes in which a response of interest is influenced by several variables, and the objective is to optimize this response. In most RSM problems, the form of the relationship between the response and the variables is unknown. Thus, an important step in RSM is to find a suitable approximation for the true functional relationship between the response (Y) and the set of independent variables (X_i) [19]. However, before applying the RSM methodology, it is necessary to define the limits of the experimental domain of the independent variables (or factors) to be explored. These limits are generally defined based on the previous available information concerning the experimental domain of the corresponding independent variables (or factors) [20–22], or limits defined by preliminary experiments in which 'one variable at a time' is varied each time, while the others are kept constant [23–25], or limits defined by a low level 'factorial design' [26]. In this work, the OVAT procedure was used as a screening design. Therefore, using the initial-rate method for the determination of hydrogen peroxide, the corresponding critical variables and their ranges were first determined based on a preliminary OVAT approach. RSM optimization was then carried out using a rotatable central composite design (CCD) consisting of four factors at three levels with eight axial points ($\alpha = 2$) and 12 replicas at the centre point ($n_0 = 12$), to obtain an estimation of the experimental error. The design was rotatable; this means that the design had points which were equidistant from the centre. The selected runs were also randomized. This procedure comprised 36 experiments, where the experimental response data were analysed by a regression procedure based on the response surface methodology (RSM). It is known that the composite design is a useful design capable of describing curvature, which is needed to explain a non-linear variation behaviour property (i.e. the variation of enzyme activity upon changing the pH value). The model that can be fitted to a composite design is an empirical function, determined from the statistical correlation suitability of the observed responses and the experimental factors. For this purpose, a second-order polynomial model equation is usually used [19]:

$$\begin{aligned} Y &= a_0 + \sum_{i=1}^{4} a_i X_i + \sum_{i=1}^{4} a_{ii} X_i^2 + \sum_{i}^{3} \sum_{j=i+1}^{4} a_{ij} X_i X_j \\ &= a_0 + a_1 X_1 + a_2 X_2 + a_3 X_3 + a_4 X_4 + a_{11} X_1^2 + a_{22} X_2^2 + a_{33} X_3^2 + a_{44} X_4^2 \\ &\quad + a_{12} X_1 X_2 + a_{13} X_1 X_3 + a_{14} X_1 X_4 + a_{23} X_2 X_3 + a_{24} X_2 X_4 + a_{34} X_3 X_4, \end{aligned} \tag{2}$$

where Y is the predicted response (e.g. initial rate of quinoneimine complex production), and X_1 (pH), X_2 (buffer concentration), X_3 (4-AAP concentration), and X_4 (T) are the independent variables or the experimental factors. The linear coefficients

a_1, a_2, a_3, and a_4 express the linear effect of each variable; the a_{11}, a_{22}, a_{33}, and a_{44} coefficients express the quadratic effects; a_{12}, a_{13}, a_{14}, a_{23} a_{24}, and a_{34}, coefficients express interactive effects between the variables, and a_0 is a constant corresponding to the central point of experimental variables. The statistical design, data analysis, and various plots were obtained by using Minitab Statistical Software (Release 14).

4. Results and discussion

4.1 *Preliminary OVAT procedure*

The initial-rate OVAT procedures were based on the collection of experimental absorption data at $\lambda_{max} = 505$ nm, generated by the absorption of quinoneimine complex produced in the reaction. In the initial-rate method, the data collection also started 20 s after the start of the reaction with a sampling time of 1 s and during 5 min. The initial rate ($mAbs\,s^{-1}$) was determined each time by linear regression performed on the absorption data obtained 20–30 s after the start of the reaction. Based on the available data mentioned in the current commercialized diagnostic kit, the starting concentrations of reagents were chosen by supplementary preliminary tests as follows: 100 mM Tris buffer, 25 mM 4-IP, 2 mM 4-AAP, 0.1 $U\,mL^{-1}$ HRP, at $T = 25°C$, and 5 μM hydrogen peroxide. After each optimization step, the optimized parameter value was substituted for its initial value. The final results can be summarized as follows:

- The optimum OVAT concentration of tris buffer was determined to be in the range of 50–250 mM (at pH = 8), for both end-point and initial-rate methods.
- The results showed that in the optimum range of 10–40 mM, the final concentration of 4-IP does not change significantly the end-point absorbance or the initial-rate of the reaction (i.e. the corresponding responses were flat and did not show any significant variation).
- The varying concentration of 4-AAP was in the range of 0.1–8.0 mM. The obtained results show that the end-point absorbance and particularly the initial rate of the reaction are both sensitively affected by the 4-AAP concentration.
- The range of optimum HRP activity for the reaction was determined using varying volumes of an initial solution of this enzyme (5.872 $U\,mL^{-1}$) added to the reagent mixture and blank cells. The obtained OVAT results show that above 0.08 $U\,mL^{-1}$, the final activity of the HRP enzyme does not change the end-point absorbance or the initial rate of the reaction (i.e. the corresponding responses were flat and did not show any significant variation).
- The results confirmed also that the temperature of the reaction should be considered as a critical chemometric variable (with an optimum value of 35°C), in the assayed range of 20–45°C, for both initial-rate and end-point methods.

Consequently, the critical variables of Emerson–Trinder reaction along with their variation ranges were found to be: X_1 (pH), X_2 (buffer concentration), X_3 (AAP concentration), and X_4 (T). The other two parameters, HRP activity and 4-IP, were shown to be non-critical in the reaction, and their values were fixed in the middle of their corresponding optimum ranges. Effectively, OVAT results showed, above the optimum value of 0.08 $U\,mL^{-1}$, that the end-point absorbance or the initial rate

of the reaction did not change significantly (i.e. optimum range with flat responses). Consequently, an optimum fixed value of $0.12\,U\,mL^{-1}$ was selected for the final HRP activity in the subsequent chemometric analysis. Similarly, in the optimum range of 10–40 mM, the final concentration of 4-IP did not significantly change the end-point absorbance or the initial-rate of the reaction (i.e. optimum range with flat responses). Therefore, the final concentration of 4-IP was fixed at 30 mM in the chemometric analysis. It should be mentioned that the fixed concentration of the H_2O_2 in the chemometric experiments was selected, as a relatively low value (e.g. 11.4 μM), based on an OVAT calibration curve.

4.2 *Response surface methodology*

The variables (coded and non-coded values), their respective levels, and the randomized experimental design are presented in table 1. Using Minitab software, the coefficients of the empirical model equation (2) and their statistical characteristics were evaluated (see table 2). Table 2 also presents the resulting estimation for the regression coefficients of the model. The results show that the factors affect the response (initial rate) in the following order: pH > AAP > T > BufC. The estimated value of the determination coefficient (R^2), expressed as a percentage, indicates that the model fits 84.1% of the experimental raw data. The fact that the R^2(adj.) value is also relatively close to the R^2 value is a conformation that there is not a necessity for a significant correction regarding the sample size and the number of terms in the model.

The quality of the regression, estimated by the analysis of variance (ANOVA), is shown in table 3. The Fisher variance ratio (F-value) is the ratio of the mean square due to regression, divided by the mean square due to error. The mean squares are obtained by dividing the sum of squares of each of the two sources of variation (the model and the error variance) by the respective degrees of freedom. If the model is a good predictor of the experimental data, the computed F-value would be higher than the tabular F-value. The evaluated values from the ANOVA table for the quadratic response function demonstrate that the model is highly significant, as the computed F-value (=7.93) is greater than the tabular F-value (=2.76) at the 5% level. The significance of the model is also confirmed for the linear, square, and interaction terms. Table 3 shows also that, in the model, the resulting 'lack of fit F-value' (=0.61) is also not very significant. Generally, the p-levels can be used as a tool to check the significance of each of the regression coefficients. This information is necessary to explain the correlation of the mutual interactions between the factors. The smaller the magnitude of the P, the more significant is the corresponding coefficient. The p-values in the table 3 reveal that all linear, square, and interaction terms are significant (at the $\alpha = 0.05$ level), and so the model confirms the presence of curvature in the response surface. The p-values for the regression (table 3) confirm, once again, the adequacy of the model.

The plot of the residuals (difference between the observed and fitted values) *versus* the randomized run order presents a completely random pattern and does not show any systematic effects or unusual observations (see figure 1). The plot of residuals versus the fitted values (see figure 2) also confirms a reasonable random distribution of the residuals around the zero line. The residual values obtained for the centre point also illustrate, in figure 2, the precision of the measurements. The linear trend of the normal plot (figure 3) and the relatively bell-shaped tendency of the residuals (figure 4) also

Table 1. Design table showing the randomized run order of experiment, and the coded and uncoded values of the different variables in the experimental design for the determination of modelled response (equation (2)).

Run order	X_1	X_2	X_3	X_4	X_1 pH	X_2 BufC (mM)	X_3 4-AAP (mM)	X_4 T (°C)
1	0	0	−2	0	8	150	1	35
2	−1	−1	1	1	7	100	4	40
3	1	1	−1	−1	9	200	2	30
4	1	−1	1	1	9	100	4	40
5	0	0	0	0	8	150	3	35
6	0	0	0	2	8	150	3	45
7	1	1	1	1	9	200	4	40
8	−1	−1	−1	1	7	100	2	40
9	2	0	0	0	10	150	3	35
10	−1	1	−1	1	7	200	2	40
11	0	0	0	0	8	150	3	35
12	−1	1	−1	−1	7	200	2	30
13	1	1	−1	1	9	200	2	40
14	−1	1	1	1	7	200	4	40
15	0	0	0	0	8	150	3	35
16	1	−1	−1	−1	9	100	2	30
17	0	0	0	0	8	150	3	35
18	0	0	2	0	8	150	5	35
19	0	0	0	0	8	150	3	35
20	−1	1	1	−1	7	200	4	30
21	0	0	0	−2	8	150	3	25
22	0	0	0	0	8	150	3	35
23	0	−2	0	0	8	50	3	35
24	−2	0	0	0	6	150	3	35
25	0	0	0	0	8	150	3	35
26	−1	−1	−1	−1	7	100	2	30
27	0	0	0	0	8	150	3	35
28	0	0	0	0	8	150	3	35
29	0	2	0	0	8	250	3	35
30	−1	−1	1	−1	7	100	4	30
31	0	0	0	0	8	150	3	35
32	1	−1	−1	−1	9	100	4	30
33	1	−1	−1	1	9	100	2	40
34	0	0	0	0	8	150	3	35
35	1	1	1	−1	9	200	4	30
36	0	0	0	0	8	150	3	35

confirm the fairly normal character of the residuals. Figure 5(a–f) show the various three-dimensional plots of the response surface model. These plots are useful to visualize the generated response surfaces by the model. A point of maximum response could mathematically be determined by partial derivatives of the generated response model equation with respect of each of the corresponding variable (factor). In matrix notation, the derivative of the quadratic model equation (Y) with respect to the elements of the vector $\mathbf{x}$ equated to zero is

$$\left(\frac{\partial Y}{\partial \mathbf{x}}\right) = \mathbf{a} + 2\mathbf{A}\mathbf{x} = 0, \tag{3}$$

where $\mathbf{a}$ is a vector of the first-order coefficients, $\mathbf{A}$ is a symmetric matrix whose main diagonal elements are the pure quadratic coefficients and whose off-diagonal elements are half the mixed quadratic coefficients, and all coefficients correspond to the

Table 2. Statistical evaluation of regression coefficients for the quadratic response (equation (2)).

Term	Coefficient	SE coefficient	*T*	*P*
Constant	−0.02981	0.014100	−2.114	0.047
X_1 (pH)	0.00753	0.002129	3.535	0.002
X_2 (BufC)	0.00012	0.000036	3.289	0.003
X_3 (AAP)	0.00538	0.001805	2.980	0.007
X_4 (T(°C))	−0.00076	0.000409	−1.857	0.077
X_1^2 (pH ∗ pH)	−0.00050	0.000108	−4.653	0.000
X_2^2 (BufC ∗ BufC)	0.00000	0.000000	−3.515	0.002
X_3^2 (AAP ∗ AAP)	−0.00050	0.000108	−4.607	0.000
X_4^2 (T ∗ T)	0.00001	0.000004	3.395	0.003
X_1X_2 (pH ∗ BufC)	0.00000	0.000003	−0.714	0.483
X_1X_3 (pH ∗ AAP)	−0.00025	0.000152	−1.618	0.121
X_1X_4 (pH ∗ T)	0.00004	0.000030	1.289	0.211
X_2X_3 (BufC ∗ AAP)	0.00001	0.000003	3.474	0.002
X_2X_4 (BufC ∗ T)	0.00000	0.000001	−4.098	0.001
X_3X_4 (AAP ∗ T)	−0.00006	0.000030	−2.127	0.045
SE = 0.0006088				
R^2 = 84.1%				
R^2 (adj.) = 73.5%				

Table 3. Statistical analysis of variance (ANOVA) for the evaluated response.

Source	df	Seq. SS	Adj. SS	Adj. MS	*F*	*P*
Regression	14	0.000041	0.000041	0.000003	7.93	0.000
Linear	4	0.000002	0.000014	0.000004	9.66	0.000
Square	4	0.000025	0.000025	0.000006	16.69	0.000
Interaction	6	0.000014	0.000014	0.000002	6.36	0.001
Residual error	21	0.000008	0.000008	0.000000		
Lack-of-fit	10	0.000003	0.000003	0.000000	0.61	0.779
Pure error	11	0.000005	0.000005	0.000000		
Total	35	0.000049				

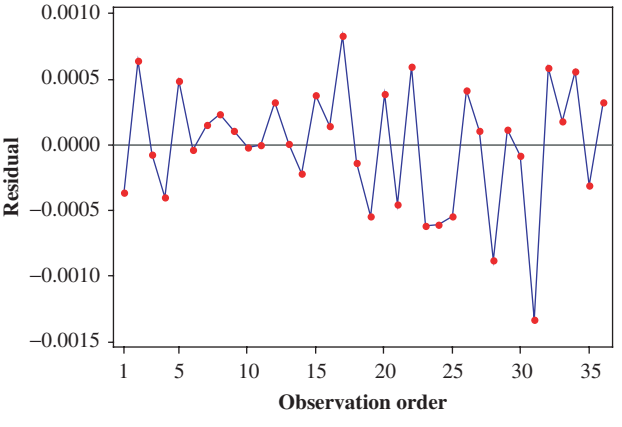

Figure 1. Residuals *vs.* randomized order of experimental runs, according to the generated design in table 1.

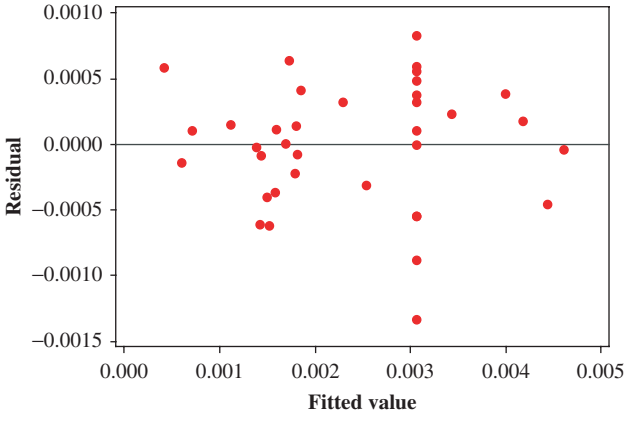

Figure 2. Residuals *vs*. fitted experimental values.

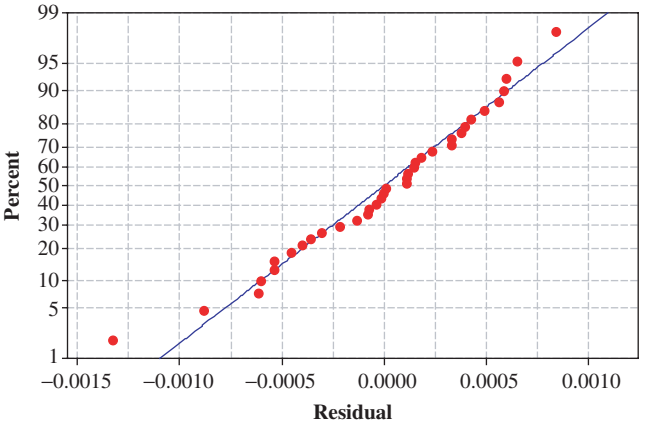

Figure 3. Normal probability plot of the residuals.

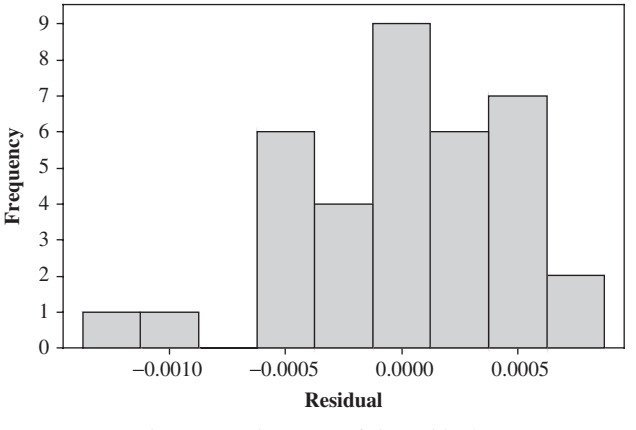

Figure 4. Histogram of the residuals.

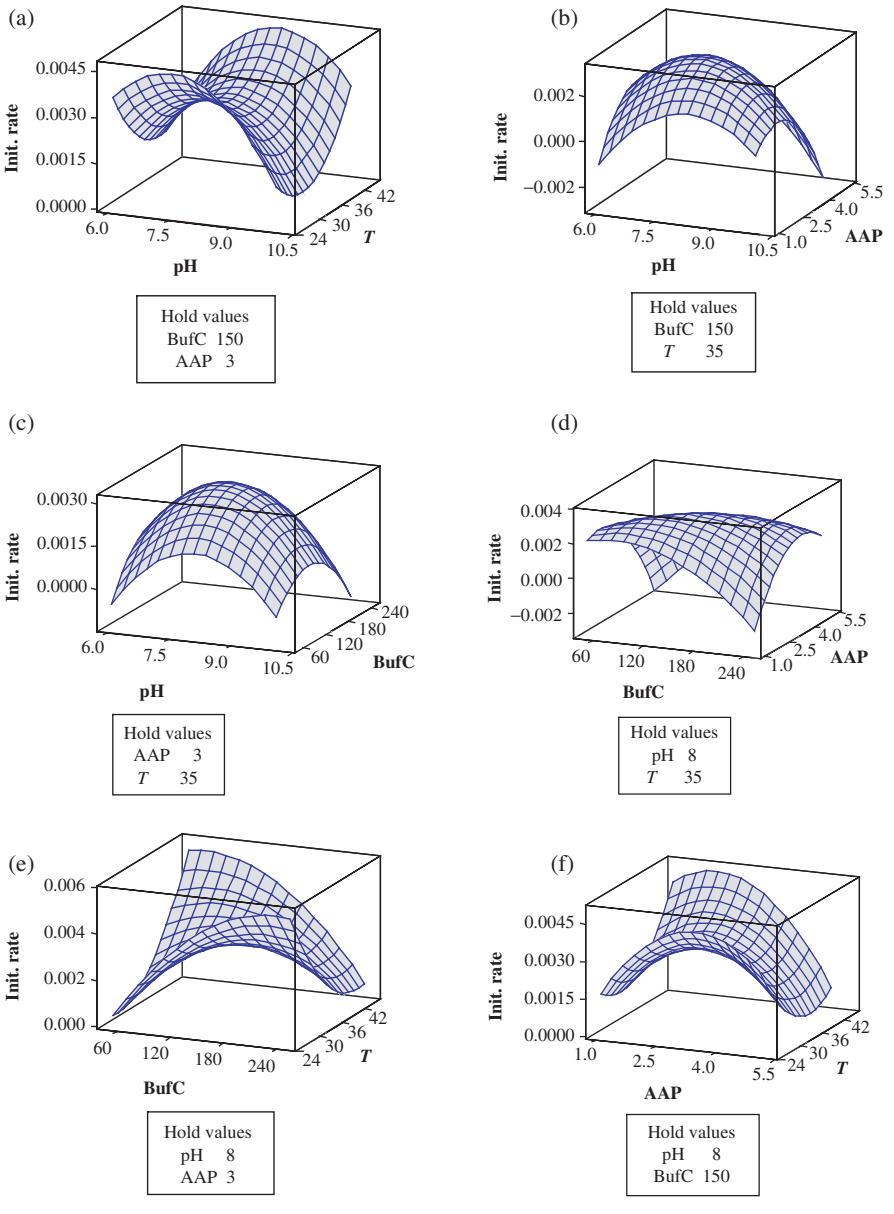

Figure 5. (a)–(f) Different three-dimensonal response surface plots. The units used in these figures are mM for reagent concentrations (AAP and BufC), and °C for temperature (T).

generated model equation, respectively. The point of maximum response ($\mathbf{x}_s$), also called the stationary point, is the solution to equation (2) [19], or

$$\mathbf{x}_s = -\frac{1}{2}\mathbf{A}^{-1}\mathbf{a}. \tag{4}$$

By the application of this mathematical method, and also by visual inspection of the 3D surface curves, the point of maximum response could be found. In our case,

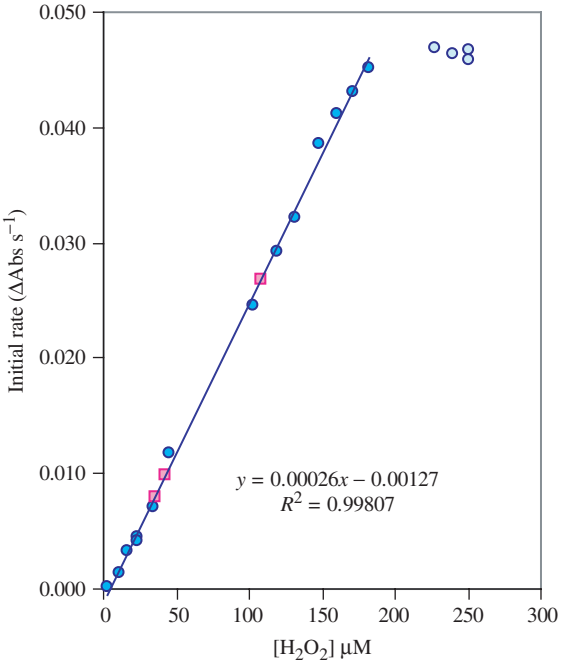

Figure 6. Calibration curve (initial rate vs. concentration) using standard aqueous H_2O_2 solutions (○) and the resulting experimental initial rate values (□) obtained for real samples using the optimized initial rate method. The data outside the linearity range are shown to illustrate the higher detection limit of the method.

the point of maximum response was found to be close to the following values: pH = 8, $T = 26°C$ (and 43°C), AAP = 3 mM, and BufC = 150 mM. However, according to the resulting RSM model equation (2) and the corresponding coefficients (table 2), the use of the standard value of $T = 25°C$ (instead of $T = 26°C$) reduces the response by only 0.6%. Therefore, for practical reasons, the value of $T = 25°C$, along with other optimum parameter values (pH = 8, AAP = 3 mM, and BufC = 150 mM), was considered for the subsequent validation of the reaction and its application for the assay of H_2O_2 in real samples.

4.3 *Test of optimized reaction*

The linear range of the method was determined by a calibration curve (initial rate *vs.* H_2O_2 concentration; see figure 6). The performance of the optimized reaction (scheme 1) was also checked by the determination of H_2O_2 in cosmetic commercial samples consisting of peroxide oxidant (hair-bleaching) creams and lotions (see section 2.2, for the declared compositions of the real samples). These samples were first diluted in doubly distilled water, and their H_2O_2 contents were determined (see figure 6 and table 4).

In addition, using another halogenated phenol (i.e. 4-fluorophenol instead of 4-iodophenol), the H_2O_2 content in these samples was also determined by this method in the same condition. The corresponding H_2O_2 values with these two

Table 4. Analytical characteristics of the optimized initial-rate enzymatic assay of H_2O_2.

Linear range (*M*)	5×10^{-6}–1.85×10^{-4} $Y = 2.6 \times 10^{-4}$X–1.27×10^{-3} $R^2 = 0.99807$	
Within-day precisions (%*RSD*)		
Aqueous samples, $N = 10$ replica		
Low: 4.89×10^{-5} M	2.83%	
High: 1.29×10^{-4} M	1.43%	
Real sample (cream), $N = 8$ replica		
3.1×10^{-5} M	2.25%	
Pool serum recovery		
Added (%)	Recovered (%)	
20, 40, 60, 80, 100	101.98, 101.36, 100.95, 102.54, 98.67	
H_2O_2 *in real samples* (*hair bleaching lotions*)		
Declared (%)	Found (%) (4-Iodophenol)	Found (%) (4-Fluorophenol)
S1 (Wella) = 9	6.77	6.91
S2 (Atousa) = 9	8.24	8.11
S3 (Igora) = 6	5.37	5.04

halogenated phenols, along with the declared manufacturer values, are presented in table 4. Although, due to the instable character of H_2O_2, the determined H_2O_2 values are systematically lower than those declared for these commercial samples, the correlation between the results obtained by these two halogenated phenols is satisfactory. It should be mentioned that these values compare well with those previously reported for such commercial samples [27]. The reported data in table 4 confirm also that the recovery of the optimized reaction for the assay of H_2O_2 is also satisfactory in human serum matrix (e.g. clinical pooled human serum samples). All other evaluated analytical characteristics (linear range, repeatability) are also reported in table 4.

5. Conclusion

Using RSM, it was possible to determine optimal experimental conditions for the indicator Emerson–Trinder (scheme 1) via an initial-rate spectophotmetric detection of the quinoneimine complex produced by the oxidative condensation of 4-iodophenol hydrogen donor with 4-aminoantipyrine. The non-linear nature of the modelled response for this system was explained by a second-order polynomial equation (see equation (2)). This methodology, as a whole, proved to be quite adequate for the design and optimization of the reaction and helped to explain the importance of the factors, their interactions, and their optimum values. In order to check the quality of the optimization, assays of H_2O_2 were performed on cosmetic samples, and also on a human pooled serum matrix. Table 4 summarizes the satisfactory analytical characteristics of the optimized procedure such as: (1) the linear range of the method (including the regressed equation of the calibration curve and its coefficient of determination); (2) within-day precisions for low and high contents of H_2O_2 in aqueous samples; (3) within-day precisions in typical cosmetic samples (along with their

corresponding numbers of replicas); (4) recovery of the method (or the matrix effect) in pooled serum samples; (5) results concerning the determination of the amount of H_2O_2 found in cosmetic samples. This optimized method benefits, both, from the analytical advantages of the spectrophotometric method (precision, recovery, selectivity) and from those associated with the kinetics initial-rate method (rapidity and sensitivity).

References

[1] P. Trinder. *Ann. Clin. Biochem.*, **6**, 24 (1969).
[2] D. Barham, P. Trinder. *Analyst*, **97**, 142 (1972).
[3] E. Emerson. *J. Org. Chem.*, **8**, 417 (1943).
[4] M.B. Ettinger, C.C. Ruchhoft, R.J. Lishka. *Anal. Chem.*, **23**, 1783 (1951).
[5] Y. Fiamegos, C. Stalikas, G. Pilidis. *Anal. Chim. Acta*, **467**, 105 (2002).
[6] N. Singh, J. Singh. *Prep. Biochem. Biotechnol.*, **32**, 127 (2002).
[7] C.A. Burtis, E.R. Ashwood. *Tietz Textbook of Clinical Chemistry*, 2nd Edn, Saunders, Philadelphia, PA (1994).
[8] P. Kabasakalian, S. Kalliney, A. Westcott. *Clin. Chem.*, **19**, 522 (1973).
[9] C.C. Allain, L.S. Poon, C.S.G. Chan, W. Richmond, P.C. Fu. *Clin. Chem.*, **20**, 470 (1974).
[10] K. Bauer. *J. Clin. Chem. Clin. Biochem.*, **19**, 971 (1981).
[11] P. Fossati, L. Prencipe. *Clin. Chem.*, **28**, 2077 (1982).
[12] F. Wang, Y.Z. Wu, X.W. Wu, S.-S. Shong, Y.X. Ci. *J. Anal. Chem.*, **344**, 556 (1992).
[13] S. Klose, M. Stoltz, E. Munz, R. Portenhauser. *Clin. Chem.*, **24**, 250 (1978).
[14] P. Fossati, L. Prencipe, G. Berti. *Clin. Chem.*, **26**, 227 (1980).
[15] K. Tamaoku, Y. Murao, K. Akiura. *Anal. Chim. Acta*, **136**, 121 (1982).
[16] F. Deyhimi, R. Salamat-Ahangari. *Talanta*, **61**, 493 (2003).
[17] J. Putter. In *Methods of Enzymatic Analysis*, H.U. Bergmeyer (Ed.), pp. 685–690, Verlag Chemie, Weinheim & Academic Press, London (1974).
[18] P. George. *Biochem. J.*, **54**, 267 (1953).
[19] D.C. Montgomery. *Design and Analysis of Experiments*, 5th Edn, Wiley, New York (2001).
[20] C.-J. Shieh, S.-W. Chang. *J. Agric. Food Chem.*, **49**, 1203 (2001).
[21] J.-H. Kwon, J. Belanger, J.R.J. Pare. *J. Agric. Food Chem.*, **51**, 1807 (2003).
[22] D. Garrido-Vidal, C. Pizarro, J.M. Gonzalez-Saiz. *Biotechnol. Prog.*, **19**, 1468 (2003).
[23] A. Bota, F.-J. Gella, F. Canalias. *Clin. Chim. Acta*, **290**, 145 (2000).
[24] E. Giraud, C. Luttmann, F. Lavelle, J.-F. Riou, P. Mailliet, A. Laoui. *J. Med. Chem.*, **43**, 1807 (2000).
[25] H. Boyaci. *Biochem. Eng. J.*, **25**, 55 (2005).
[26] G.A. Macedo, GM. Pastore, M.I. Rodrigues. *Process Biochem.*, **39**, 687 (2004).
[27] L. Camparella, R. Roversi, M.P. Sammartino, M. Tomassetti. *J. Pharmaceut. Biomed. Anal.*, **18**, 105 (1998).